

# PERFORMANCE OF TEXTURED TOOL IN TURNING OF NIMONIC 80A UNDER MINIMUM QUANTITY LUBRICATION

<sup>1</sup>J Sai Kumar and <sup>2</sup>Dr.P.Prasanna, <sup>3</sup>P. Mallikarjuna, <sup>4</sup>A.Seshappa

<sup>1</sup>Post Graduate Student,<sup>3,4</sup>Research scholar,<sup>2</sup>Associate Professor of Mechanical Engineering  
JNTUH University College of Engineering, Science and Technology Hyderabad, India.

**ABSTRACT:** This research delves into the machinability concerns of Nimonic 80A, a nickel-based superalloy that finds widespread use in aircraft. The high temperature at the tool-workpiece contact causes rapid acceleration of tool wear, making Nimonic 80A a challenging material to fabricate. The research looks at the effectiveness of combining tool texturing with minimum quantity lubrication (MQL) to improve machining efficiency. To find out how these approaches work, we measure important performance indicators, including cutting temperature, surface quality, and tool wear. To optimize the process parameters, the experimental design employs Grey Relational Analysis (GRA). The research evaluates several tool geometries to find the optimal configuration for improving surface quality and decreasing wear. Texturing tools may make them cooler and more lubricated, reducing heat production. We investigate MQL, a lubrication method that reduces coolant consumption since it has the ability to lessen friction and enhance cutting conditions. The combination of tool texturing with MQL resulted in lower cutting temperatures and decreased tool wear, according to the experimental findings. Based on the results, it seems like a good idea to combine these two methods to make Nimonic 80A more machined for use in aerospace.

**Key Words** – Nimonic 80A, Circular Pit Hole Tool Insert, Minimum Quantity Lubrication, Taguchi Method, Grey Relational Analysis.

## I. INTRODUCTION

High production rates, environmental sustainability, and operator safety are some of the problems of machining tough-to-cut materials. Tool life and performance may be negatively affected by heat generation in chips, cutting tools, and machined surfaces. A number of factors go into temperature control, including tool design, cooling methods, and ideal cutting conditions. By reducing friction, enhancing lubrication, and minimising tool wear, textured cutting tools with micro- or nanoscale surface patterns might enhance MQL-assisted turning operations on materials like Nimonic 80A. Some materials are notoriously tough to machine, such as heat-resistant superalloys, composites, titanium alloys, and hardened steels. The material removal rates, surface polish, and tool wear in these materials are already poor, and concerns with workpiece stability, high cutting temperatures, and poor chip removal further make things worse. Nontraditional, hard-to-machine materials can provide significant challenges. This research looks at how well carbide tools with micro-dimple and micro-channel textures spin when dry. Results show that micro-channel tools increase tool life at slower speeds while evaluating Inconel 718. Conversely, micro-dimple tools provide better surface quality with less cutting effort. For better machinability, they also recommend further study of hybrid micro-textured designs[1]. Compared to traditional dry and wet turning, this study demonstrates that cryogenic turning of Inconel 718 improves tool life by 133%, reduces energy usage by 8–17%, and reduces surface roughness by 20–37%, highlighting its potential to replace less environmentally friendly machining techniques [2]. Tool life, cutting energy, and surface roughness are compared to Minimum Quantity Lubrication (MQL) to evaluate a new Electrostatic Minimum Quantity Lubrication (EMQL) nozzle design for end milling Inconel 718 [3]. Compared to dry cutting and MQL, NFMQL significantly improves surface roughness and topography while reducing tool wear, according to a study on AA 2024 T3 Al alloy machining using different cooling/lubrication techniques (dry cutting, MQL, and MoS<sub>2</sub> nanofluid MQL)[4]. Research comparing MQL and dry cutting on AISI D2 cold work tool steel demonstrates that MQL reduces tool wear, cutting temperature, and vibration amplitude by 23%, 25%, and 45%, respectively, while improving surface roughness by 89% and extending tool life by up to 267% [5]. evaluated of MQL+nanofluid (MQL+Nano) with traditional MQL, MQL with wheel cleaning jet (MQL+WCJ), and flood cooling shows that while MQL+Nano enhances surface quality and reduces grinding power, MQL+WCJ delivers the best performance in terms of surface quality, wheel wear, and roundness error, offering environmental and health benefits [6]. Effected to different cooling-lubrication methods (dry cutting, nitrogen cooling, N<sub>2</sub>MQL, and Ranque–Hilsch vortex tube N<sub>2</sub>MQL) on the machining of Al 7075-T6 alloy found that R-N2MQL can reduce surface roughness by up to 77%, tool wear by up to 118%, and promote sustainability by improving chip management and reducing waste [7]. Investigated on micro-textured tools for machining GH4169 nickel-based superalloy with spray cooling optimizes tool shape, size parameters, and cutting

conditions through simulations and experiments, improving cutting performance and guiding micro-textured tool design for efficient machining [8]. Studied on solid lubricant-assisted machining (SLAM) of AISI 52100 steel shows significant improvements over dry machining, with reductions of 45-60% in cutting forces, 14-29% in vibration acceleration, 11-17% in tool wear, and enhancements of 47-66% in surface finish [9]. The impact of cutting speed on tool wear in turning Inconel 657 shows that carbide tools perform better at low speeds, while CBN tools excel at higher speeds, with CBN exhibiting up to 39% less wear than carbide at 60 m/min and 35% less at 120 m/min [10]. The effect of surface texturing on heat transfer in machining tools shows that grooves of varying depths (50, 100, 150 μm) increase heat transfer, with a 3.77% improvement for a 150 μm depth, due to enhanced contact area, fluid turbulence, and surface wettability [11]. Parallel Grooved Textured Tools (PGT) for machining EN24 alloy steel under Minimum Quantity Lubrication (MQL) conditions demonstrate that PGTs reduce cutting temperature, rake wear, flank wear, surface roughness, and cutting force by up to 18.96%, 18.79%, 24.31%, 12.69%, and 18.96%, respectively, compared to un-textured tools [12]. Investigated the performance of textured tools in the turning of superalloys using minimum quantity lubrication (MQL). The results are compared to untextured tools for the same superalloys to understand the effect of surface texture on machining efficiency. Key performance metrics, including cutting temperature, surface roughness, and tool rake wear, are assessed for both textured and untextured tool inserts. The findings provide insights into how textured tools influence the machining process and tool wear under MQL conditions.

**II. EXPERIMENTAL PROCEDURE**

The nickel-based super alloy known as NIMONIC 80A is recognized for the exceptional mechanical qualities it has even when subjected to high temperatures. In situations where exceptional strength, resistance to oxidation, and resistance to corrosion are needed, this alloy is quite often utilised. Due to the features that it has, it is ideal for usage in components that are used in gas turbines and airplanes, in addition to other demanding environments. Even at high temperatures, the alloy is able to keep its structural integrity, often about 1000 degrees Celsius (1830 degrees Fahrenheit). The development of a protective oxide layer, which increases its resistance to oxidation, is another beneficial effect. In addition, NIMONIC 80A has outstanding creep resistance, which enables it to endure deformation even when subjected to stress over an extended period of time. Although traditional welding procedures may be used to join the alloy, particular care must be taken to ensure that its qualities are not compromised. Making a machine out of NIMONIC 80A may be difficult because of its hardness, and it often requires the use of specialized equipment. This super alloy is held in high esteem by several industries because to its dependability and performance in harsh environments. All things considered, NIMONIC 80A is an essential material in engineering domains that involve significant risks. Additionally, the chemical composition of the NIMONIC 80A alloy as well as its mechanical properties are shown in Tables 1 and 2.

**Table 1.** Chemical composition of the NIMONIC 80A (%)

Weight%	Ag	Pb	B	S	C	Cu	Si	Mn	Fe	Al	Co	Ti	Cr	Ni
Alloy 80	0.0005 max	0.0020 max	0.008 max	0.015 max	0.10 max	0.2 max	1.0 max	1.0 max	1.5 max	1.80	2	2.70	21	Bal

**Table 2.** Mechanical Properties of the NIMONIC 80A

Material	Temperature (°C)	Yield Strength (MPa)	Tensile Strength (MPa)	Elongation (%)	Hardness
Nimonic 80A Bar Solution Treated	Room Temperature	-	-	-	295 max
Nimonic 80A Bar Treated	Room Temperature	695 min	1080 min	20 min	310 min
Nimonic 80A Bar Treated	500	672	1038	31	-

The L9 orthogonal array design is a statistical approach utilized in experiments to analyze the impact of several factors while minimizing the number of trials. It includes 9 experimental runs and can handle up to 4 factors, each set at 3 different levels, facilitating effective investigation of variable interactions. This design is especially valuable in quality enhancement and optimization research, offering a systematic way to determine the best conditions for a given process. By considering process parameters experimental design is mentioned in Table. 3. Following the completion of the machining operation, the performance of the circular pit hole tool insert and the plane cutting tool insert is evaluated by comparing their reactions. Minitab will be used for additional analysis in order to determine the best machining parameters for both tool inserts. To comprehend how various parameters affect machining performance, a thorough analysis of the comparison's data will be conducted. The best values for each parameter will be found by applying Grey Relational Analysis (GRA) optimization on both

tool inserts. The goal of this optimization procedure is to improve cutting performance and tool wear while also increasing machining efficiency.

**Table 3.** Experimental Plan based on Taguchi L<sub>9</sub> Orthogonal Array

Exp. runs	Process Parameters		
	Cutting speed(rpm)	Feed rate (mm/rev)	Depth of cut(mm)
1	600	0.1	0.2
2	600	0.15	0.4
3	600	0.2	0.6
4	920	0.1	0.4
5	920	0.15	0.6
6	920	0.2	0.2
7	1275	0.1	0.6
8	1275	0.15	0.2
9	1275	0.2	0.4

### III. RESULTS AND DISCUSSION

A plane-cutting tool insert is a crucial replaceable component used in machining to cut flat surfaces. Typically featuring a flat, straight edge, these inserts come in various shapes like rectangular and triangular, and are made from durable materials such as carbide, high-speed steel, or ceramic. These are widely employed in milling, turning, and surface finishing, allowing for efficient production of flat surfaces on metal parts. One key advantage is their quick-change capability, which reduces downtime while maintaining sharp cutting edges for improved surface finish and accuracy. Regular maintenance and timely replacement of worn inserts are essential for optimal performance and efficiency in machining operations.

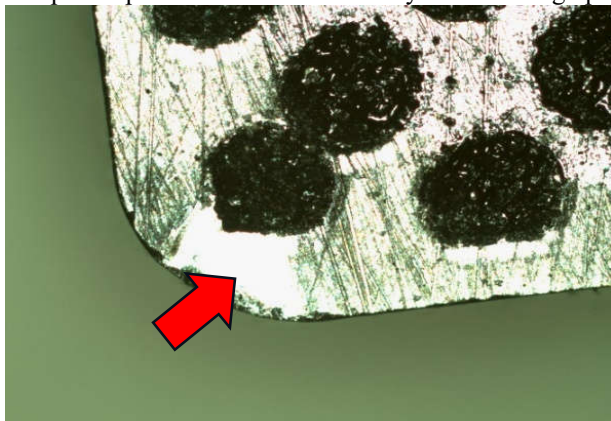


**Fig 1.** Rake Wear in Circular Pit Hole



**Fig 2.** Rake Wear in Plane Cutting Tool Insert

The tool inserts depicted in Fig 1 and Fig 2 showcase rake wear patterns for both circular pit hole inserts and plane-cutting tool inserts. Rake wear has a major effect on tool performance and longevity since it is essential to cutting effectiveness and surface finish quality. For the circular pit hole insert, wear might be less evident at certain contact points because of the insert's geometry. In contrast, the plane-cutting tool insert could show a different wear distribution, which may lead to variations in cutting forces. Studying these wear patterns is essential for enhancing tool design and material choices to improve machining operations.

The lowest cutting temperature of 173.33°C was attained by turning Nimonic 80A material with a plane cutting tool insert and little lubrication at a speed of 1275 RPM, feed rate of 0.15 mm/rev, and depth of cut of 0.2 mm. A surface roughness of 0.456 μm was achieved with the best results when the cutting speed was 920 RPM, the feed rate was 0.2 mm/rev, and the depth of cut was 0.2 mm. Furthermore, at a depth of cut of 0.2 mm, a feed rate of 0.1 mm/rev, and a cutting speed of 600 RPM, tool rake wear was recorded at 0.1809 mm.

In the turning of Nimonic 80A material with a circular pit hole textured tool insert using minimum quantity lubrication, at 600 RPM, 0.1 mm/rev feed rate, and 0.2 mm depth of cut, the lowest cutting temperature ever measured was 119°C. Under the same circumstances, the ideal surface roughness of 0.751 μm was attained. With a feed rate of 0.15 mm/rev, a depth of cut of 0.2 mm, and a cutting speed of 1275 RPM, the tool rake wear measured 0.133 mm. These results show the significance of choosing the appropriate settings for enhanced performance and decreased heat generation by illustrating how cutting parameters impact temperature, surface polish, and tool wear. Overall, this study emphasizes the need for careful parameter selection to enhance

machining efficiency and prolong tool life in processes using minimum quantity lubrication.

**Table 4.** Experimental results for Untextured Tool Insert

Untextured Tool									
Exp. runs	Process Parameters			Responses			S/N ratios of results		
	cutting speed (rpm)	feed rate (mm/rev)	depth of cut (mm)	cutting temperature (°c)	Surface roughness Ra (µm)	Tool rake wear V <sub>b</sub> (mm)	Cutting temperature T <sub>c</sub> (dB)	Surface Roughness Ra (dB)	Tool rake wear V <sub>b</sub> (dB)
1	600	0.1	0.2	202.66	0.551	<b>0.1809</b>	-46.1354	5.17697	14.8512
2	600	0.15	0.4	203.66	0.505	0.2525	-46.1781	5.93417	11.9548
3	600	0.2	0.6	227.66	1.348	0.2456	-47.1457	2.59380	12.1954
4	920	0.1	0.4	210.66	0.514	0.2083	-46.4716	5.78074	13.6262
5	920	0.15	0.6	289.00	.536	0.2916	-49.2180	5.41670	<b>10.7042</b>
6	920	0.2	0.2	210.00	<b>0.456</b>	0.2230	-46.4444	6.82070	13.0339
7	1275	0.1	0.6	249.00	0.757	0.2683	-47.9240	<b>2.41808</b>	11.4276
8	1275	0.15	0.2	<b>173.33</b>	0.521	0.1980	<b>-44.7775</b>	5.66325	14.0667
9	1275	0.2	0.4	220.33	0.738	0.2463	-46.8615	2.63887	12.1707

**Table 5.** Experimental results for Textured Tool Insert

Circular Pit hole Textured Tool									
Exp. runs	process parameters			Experimental results			S/N ratios of results		
	Cutting Speed (rpm)	Feed rate (mm/rev)	Depth of cut (mm)	Cutting Temperature (°c)	Surface Roughness Ra (µm)	Tool rake wear V <sub>b</sub> (mm)	Cutting Temperature T <sub>c</sub> (dB)	Surface Roughness Ra (dB)	Tool rake wear V <sub>b</sub> (dB)
1	600	0.1	0.2	<b>119.00</b>	<b>0.751</b>	0.178	-41.5109	2.48720	14.9916
2	600	0.15	0.4	135.50	0.808	0.218	-42.6388	1.85177	13.2309
3	600	0.2	0.6	131.75	0.769	0.192	-42.3950	2.28147	14.3340
4	920	0.1	0.4	191.33	1.115	0.279	-45.6357	-0.94550	11.0879
5	920	0.15	0.6	184.66	0.927	0.292	-45.3275	0.65841	10.6923
6	920	0.2	0.2	140.66	0.915	0.182	-42.9634	0.77175	14.7986
7	1275	0.1	0.6	267.66	0.920	0.208	-48.5517	0.72424	13.6387
8	1275	0.15	0.2	206.33	1.034	<b>0.133</b>	-46.2912	-0.29041	17.5230
9	1275	0.2	0.4	221.33	0.813	0.232	-46.9008	1.79819	12.6902

The tables present a comparison of experimental results for Untextured Tool Inserts (Table 4) and Circular Pit Hole Textured Tool Inserts (Table 5) based on process parameters, responses, and signal-to-noise (SN) ratios. Both tools are evaluated under similar process conditions, with cutting speeds ranging from 600 to 1275 rpm, feed rates from 0.1 to 0.2 mm/rev, and depths of cut between 0.2 and 0.4 mm. For untextured tools, cutting temperatures vary from 202.66 to 249.00°C, surface roughness (Ra) ranges from 0.456 to 0.738 µm, and tool rake wear (V<sub>b</sub>) is between 0.1809 and 0.2463 mm. The optimal SN ratios for surface roughness and tool wear are achieved with low

cutting speed, feed rate, and depth of cut. On the other hand, textured tools show better-cutting temperature management (119.00–221.33°C) and reduced tool wear ( $V_b$ : 0.133–0.279 mm), although their surface roughness values are slightly higher ( $R_a$ : 0.751–1.115  $\mu\text{m}$ ). Overall, textured tools perform better in reducing tool wear and managing heat, while untextured tools achieve superior surface quality under low cutting speed and depth of cut. The ideal process parameters for minimizing flaws vary between the two types of tools.

### III.I. Effect of Process Parameters on Each Response for Untextured Tool

An effective way to improve machining operations is to use Minitab's Taguchi method to examine experimental data on cutting temperature, surface roughness, and tool rake wear. This method helps determine the best machining parameters to reduce variability and improve quality. High cutting temperatures can hurt workpiece quality and tool life. While Minitab's tools facilitate variance analysis to pinpoint important influences on surface quality and tool wear, Taguchi's sturdy design makes it possible to evaluate variables like cutting speed, feed rate, and depth of cut. In the end, this analysis leads to better machining conditions, increasing productivity and product quality by making data-driven, well-informed decisions.

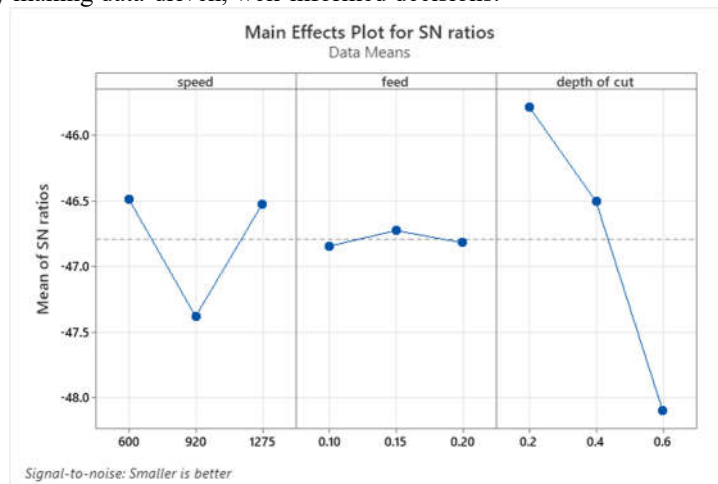


**Fig 3.** Effect of Cutting Speed, Feed Rate, and Depth of Cut on Cutting Temperature under MQL for Plane Cutting Tool Insert

The Main Effects Plot for SN Ratios reveals that speed and depth of cut have a substantial influence on the SN ratio. The levels with the lowest values (600 for speed and 0.2 for depth of cut) achieve the highest performance when compared to the "Smaller is Better" criteria. As can be seen in Figure 3, feed, on the other hand, has no impact on the SN ratio throughout all of its levels.

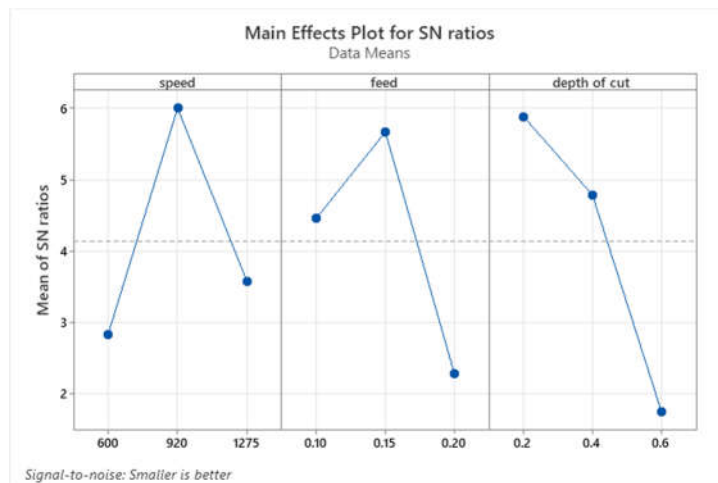


**Fig 4.** Effect of Cutting Speed, Feed Rate, and Depth of Cut on Surface Roughness under MQL for Plane Cutting Tool Insert

To reduce SN ratios under the "Smaller is better" criterion, the Main Effects Plot for SN Ratios assesses the effects of Speed, Feed, and Depth of Cut. According to speed, the highest (unwanted) SN ratio is produced at 920, while the lowest SN ratio is found at 1275. The most advantageous SN ratio for feed is 0.20, which is also the lowest. There is a discernible pattern in Depth of Cut, with the lowest value (0.2) consistently producing the lowest SN ratio. According to these results, the best parameters for improved performance are Speed: 1275, Feed: 0.20, and Depth of Cut: 0.2, as illustrated in Fig 4.

The graph above, labeled "Main Effects Plot for SN Ratios," uses the adage "Smaller is Better" to analyzed the relationship between the response variable and the variables of speed, feed, and depth of cut. The data shows that the optimum performance, as shown by the best SN ratios (0.2), is achieved at lower depths of cut (0.2), feed (0.10), and speeds (600). This information is presented in Figure 5.

The signal-to-noise ratio for the smaller the better =  $-10 \log_{10} \frac{1}{n} \sum (R)^2$  (1)

Where, n = No. of observations, R = Observed data for each response



Fig 5. Effect of Cutting Speed, Feed Rate, and Depth of Cut on Tool Rake Wear under MQL for Plane Cutting Tool Insert

In the same way, the Signal to Noise (S/N) ratios at each level can be computed as illustrated previously. These calculations follow a consistent methodology. The resulting S/N ratios are then organized for clarity. They are displayed in both Fig. 3, 4, and 5. This presentation allows for straightforward comparison and analysis of the data.

Table 6. Mean S/N ratio response table for Cutting Temperature

Symbol	Process parameters	Mean S/N ratio				
		Level 1	Level 2	Level 3	Max-Min	Rank
v	Cutting speed (rpm)	-46.49	-47.38	-46.52	0.89	2
f	Feed rate (mm/rev)	-46.84	-46.72	-46.82	0.12	3
d	Depth of cut (mm)	-45.79	-46.50	-48.10	2.31	1

Table 7. ANOVA of Cutting Temperature for Untextured Tool

Source	Degree of freedom	Sum of squares	Mean squares	% contribution
v	2	1.5306	0.76530	12.357
f	2	0.0235	0.01174	0.189
d	2	8.3873	4.19364	67.71
Residual error	2	2.4450	1.22248	19.73
Total	8	12.3863		100

Table 8. Mean S/N ratio response table for Surface Roughness

Symbol	Process parameters	Mean S/N ratio				
		Level 1	Level 2	Level 3	Max-Min	Rank
v	Cutting speed (rpm)	2.839	6.006	3.573	3.167	3
f	Feed rate (mm/rev)	4.459	5.671	2.289	3.383	2
d	Depth of cut (mm)	5.887	4.785	1.747	4.140	1

Table 9. ANOVA of Surface Roughness for Untextured Tool

Source	Degree of freedom	Sum of squares	Mean squares	% contribution
v	2	16.486	8.243	24.00
f	2	17.623	8.811	25.65
d	2	27.582	13.791	40.15
Residual error	2	6.994	3.497	10.18
Total	8	68.685		100

**Table 10.** Mean S/N ratio response table for Tool Rake Wear

Symbol	Process parameters	Mean S/N ratio				
		Level 1	Level 2	Level 3	Max-Min	Rank
v	Cutting speed (rpm)	13.00	12.45	12.55	0.55	3
f	Feed rate (mm/rev)	13.30	12.24	12.47	1.06	2
d	Depth of cut (mm)	13.98	12.58	11.44	2.54	1

**Table 11.** ANOVA of Tool Rake Wear for Untextured Tool

Source	Degree of freedom	Sum of squares	Mean squares	% contribution
v	2	0.5063	0.2531	3.57
f	2	1.8709	0.9354	13.22
d	2	9.7224	4.8612	68.71
Residual error	2	2.0496	1.0248	14.48
Total	8	14.1491		100

The percentage contribution of each process parameter to cutting temperature, surface roughness, and tool rake wear is calculated using Tables 7, 9, and 11. The calculation of these percentage contributions is outlined in the following sections. By analyzing the data, we can quantify the influence of each parameter. This approach helps in understanding how each factor contributes to the overall cutting temperature. The percentages that are produced offer important information for process optimization.

Sample Calculation of Cutting Temperature for Untextured Tool:

$$\% \text{ contribution for cutting speed (v)} = \frac{\text{Sum of squares}}{\text{Total}} \tag{2}$$

$$\% \text{ contribution for feed rate (f)} = \frac{\text{Sum of squares}}{\text{Total}} \tag{3}$$

$$\% \text{ contribution for depth of cut(d)} = \frac{\text{Sum of squares}}{\text{Total}} \tag{4}$$

$$\% \text{Error} = \frac{2.4450}{12.3863} = 19.73\%$$

Thus, the highest percentage contribution is the depth of cut, which accounts for 67.71%. Additionally, the percentage error associated with this measurement is 19.73%. These figures highlight the depth of cut significant impact on cutting temperature.

**III.II. Effect of Process Parameters on Each Response for Circular Pit Hole Tool:**

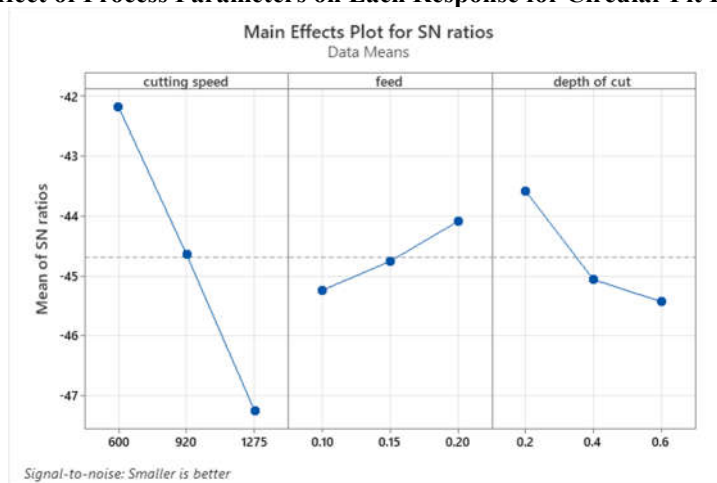


**Fig 6.** Effect of Cutting Speed, Feed Rate, and Depth of Cut on Cutting Temperature under MQL for Circular Pit Hole Tool Insert

Utilizing the "Smaller is Better" criterion, the "Main Effects Plot for SN Ratios" illustrates how cutting depth of cut, feed, and speed affect performance. Lower SN ratios indicate worse outcomes and are a result of deeper and faster cutting. A non-linear influence is seen in the feed, with an ideal value of 0.20. For reducing unpredictability or defects, the lowest cutting speed (600), maximum feed (0.20), and lowest depth of cut (0.2) are the best choices. Because they lessen the effect of undesirable changes, these features maximize performance.

Under the "Smaller is Better" criterion, which favors lower SN ratios, this "Main Effects Plot for SN Ratios" investigates the effects of cutting speed, feed, and depth of cut on SN ratios. At a medium depth of cut (0.4) and medium cutting speed (920), the SN ratio improves, and performance is stable at low feed levels (0.10 or 0.15). Figure 7 illustrates the ideal parameters for reducing unpredictability or flaws: 920 cutting speed, 0.10 or 0.15 feed, and 0.4 depth of cut.

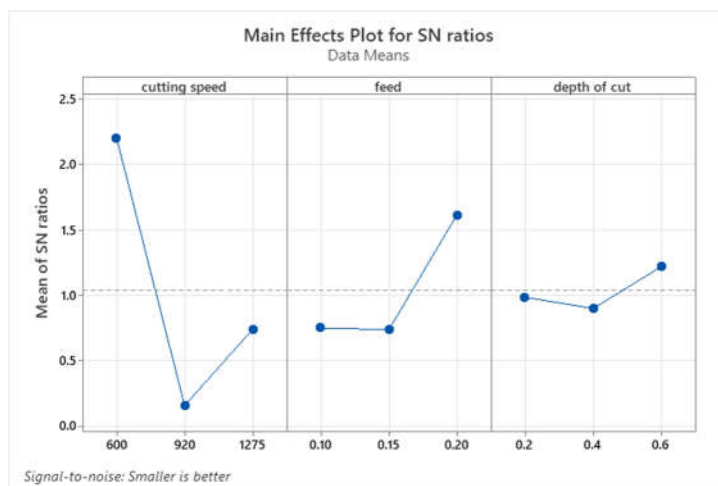


Fig 7. Effect of Cutting Speed, Feed Rate, and Depth of Cut on Surface Roughness under MQL for Circular Pit Hole Tool Insert

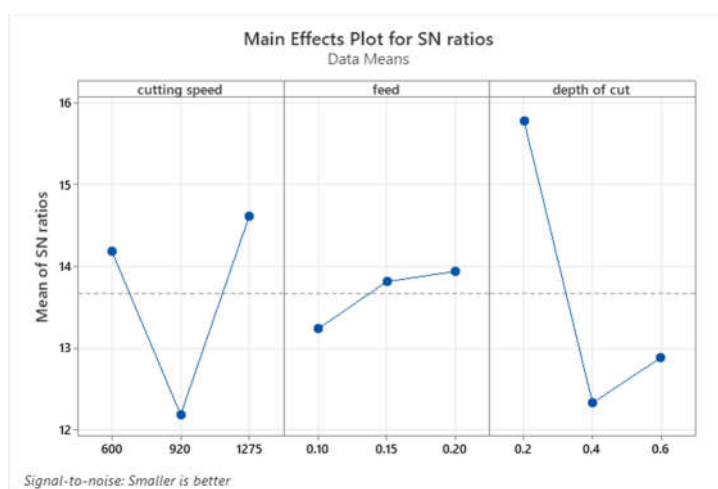


Fig 8. Effect of Cutting Speed, Feed Rate, and Depth of Cut on Tool Rake Wear under MQL for Circular Pit Hole Tool Insert

To reduce variability ("Smaller is better"), this Main Effects Plot for SN ratios illustrates how cutting speed, feed, and depth of cut affect the mean SN ratio. The most important factors are cutting speed and depth of cut; as illustrated in Fig. 8, the ideal values are 1275 for cutting speed, 0.20 for feed, and 0.2 for depth of cut.

$$\text{The signal-to-noise ratio for the smaller the better} = -10 \log_{10} \frac{1}{n} \sum (R)^2 \tag{5}$$

Where, n = No. of observations, R = Observed data for each response

Similarly, the Signal Noise (S/N) ratios at each level can be computed using the previously described method. The results are organized systematically for better clarity. Figures 6, 7, and 8 present the S/N ratios, making comparing and analyzing the data easier.

Table 12.S/N ratio response table for cutting temperature

Symbol	Process parameters	Mean S/N ratio				
		Level 1	Level 2	Level 3	Max-Min	Rank
v	Cutting speed (rpm)	-42.18	-44.64	-47.25	5.07	1
f	Feed rate (mm/rev)	-45.23	-44.75	-44.09	1.15	3
d	Depth of cut (mm)	-43.59	-45.06	-45.42	1.18	2

Table 13.ANOVA of cutting temperature for Circular Pit Hole Textured tool

Source	Degree of freedom	Sum of squares	Mean squares	% contribution
v	2	38.5121	19.2560	83.31
f	2	1.9884	0.9942	4.30
d	2	5.6663	2.8331	12.25
Residual error	2	0.0600	0.0300	0.12
Total	8	46.2267		100



**Table 14:** S/N ratio response table for surface roughness

Symbol	Process parameters	Mean S/N ratio				
		Level 1	Level 2	Level 3	Max-Min	Rank
v	Cutting speed (rpm)	2.2068	0.1615	0.7440	2.0453	1
f	Feed rate (mm/rev)	0.7553	0.7399	1.6171	0.8772	2
d	Depth of cut (mm)	0.9895	0.9015	1.2214	0.3199	3

**Table 15.**ANOVA of surface roughness for CPT tool

Source	Degree of freedom	Sum of squares	Mean squares	% contribution
v	2	6.6625	3.33123	61.12
f	2	1.5123	0.75614	13.87
d	2	0.1639	0.08193	1.50
Residual error	2	2.5604	1.28019	23.49
Total	8	10.8990		100

**Table 16.**S/N ratio response table for tool rake wear

Symbol	Process parameters	Mean S/N ratio				
		Level 1	Level 2	Level 3	Max-Min	Rank
v	Cutting speed (rpm)	14.19	12.19	14.62	2.42	2
f	Feed rate (mm/rev)	13.24	13.82	13.94	0.70	3
d	Depth of cut (mm)	15.77	12.34	12.89	3.43	1

**Table 17.**ANOVA of tool rake wear for CPT tool

Source	Degree of freedom	Sum of squares	Mean squares	% contribution
v	2	10.0343	5.0171	28.67
f	2	0.8396	0.4198	2.39
d	2	20.4118	10.2059	58.32
Residual error	2	3.7079	1.8540	10.59
Total	8	34.9937		100

Tables 13, 15, and 17 are employed to determine the percentage contribution of each process parameter to each response. The calculation of these percentage contributions is outlined in the following sections. By analyzing the data, we can quantify the influence of each parameter. This approach helps in understanding how each factor contributes to the overall cutting temperature. The resulting percentages provide valuable insights for optimizing the process.

$$\% \text{ contribution for cutting speed (v)} = \frac{\text{Sum of squares}}{\text{Total}} \tag{6}$$

$$\% \text{ contribution for feed rate (f)} = \frac{\text{Sum of squares}}{\text{Total}} \tag{7}$$

$$\% \text{ contribution for depth of cut(d)} = \frac{\text{Sum of squares}}{\text{Total}} \tag{8}$$

$$\% \text{Error} = \frac{0.06}{46.2267} = 0.12\%$$

Thus, the highest percentage contribution is attributed to the cutting speed (v), which accounts for 83.31%. Additionally, the percentage error associated with this measurement is 0.12%. These figures highlight the cutting speed (v) a significant impact on cutting temperature.

**Table 18.** Confirmation Results for Developed Models:

Responses	Plane Cutting Tool Insert		Circular Pit Hole Tool Insert	
	Prediction	Experiment	Prediction	Experiment
Cutting Temperature(°C)	189.8	187.3	93.16	91.86
Surfaceroughness (µm)	1.0238	0.893	0.8932	0.868
Tool Rake Wear (mm)	0.26859	0.256	0.223	0.213

The regression analysis results in Minitab for both the Plane Cutting Tool Insert and the Circular Pit Hole Tool Insert provide a comparison of their performance. However, to verify these results, further experimental trials must be conducted to ensure the predictions are accurate and reliable. According to the regression data, the

Circular Pit Hole Tool Insert seems to outperform the Plane Cutting Tool Insert. This indicates that the Circular Pit Hole Tool Insert could offer enhanced efficiency or quality for the given task. Consequently, additional trials are required to confirm that the observed trend is consistent under practical conditions.

#### IV. CONCLUSIONS

The following conclusions were made from this evaluation:

- Optimum Cutting condition for Plane Cutting Tool Insert Obtained at  $v = 1275$ (rpm),  $f = 0.15$  (mm/rev) and  $d = 0.2$ (mm) under Minimum Quantity Lubrication by using Grey Relational Analysis.
- Optimum Cutting condition for Circular Pit Hole Tool Insert Obtained at  $v = 600$ (rpm),  $f = 0.1$ (mm/rev), and  $d = 0.2$ (mm) under Minimum Quantity Lubrication by using Grey Relational Analysis.
- Depth of Cut is the most influencing parameter for Plane Cutting Tool Insert on Surface Roughness, Cutting Temperature, and Tool Rake Wear with a maximum contribution of 68.71%.
- The depth of cut affects Tool Rake Wear with a 58.32% contribution under Minimum Quantity Lubrication, whereas Cutting Speed is one of the factors influencing Circular Pit Hole Insert on Cutting Temperature and Surface Roughness with a contribution of 83.31% and 61.12%.
- Because the Textured Tool uses Minimum Quantity Lubrication (MQL), it produces better outcomes than the Untextured Tool. In particular, the Textured Tool has less wear on the cutting edge as indicated by the rake wear ( $V_b$ ). Less wear is indicated by the rake wear measured at  $V_b = 0.133$  mm for the CPT (Circular Pit Hole Tool) with MQL. The Untextured Tool, on the other hand, has a greater wear value of  $V_b = 0.1809$  mm. This gain is ascribed to MQL's improved cooling and lubrication, which lowers heat and friction and increases tool longevity and performance.

#### REFERENCES

- [1]. Rajurkar, Avadhoot, and Satish Chinchankar. "Experimental investigation on laser-processed micro-dimple and micro-channel textured tools during turning of Inconel 718 alloy." *Journal of Materials Engineering and Performance* (2022): 1-16.
- [2]. Khanna, Navneet, Chetan Agrawal, Manu Dogra, and Catalin Iulian Pruncu. "Evaluation of tool wear, energy consumption, and surface roughness during turning of inconel 718 using sustainable machining technique." *Journal of Materials Research and technology* 9, no. 3 (2020): 5794-5804.
- [3]. De Bartolomeis, Andrea, Stephen T. Newman, and Alborz Shokrani. "High-speed milling Inconel 718 using electrostatic minimum quantity lubrication (EMQL)." *Procedia CIRP* 101 (2021): 354-357.
- [4]. Yücel, Ayşegül, Çağrı Vakkas Yıldırım, Murat Sarıkaya, Şenol Şirin, Turgay Kıvak, Munish Kumar Gupta, and Ítalo V. Tomaz. "Influence of MoS<sub>2</sub> based nanofluid-MQL on tribological and machining characteristics in turning of AA 2024 T3 aluminum alloy." *Journal of Materials Research and Technology* 15 (2021): 1688-1704.
- [5]. Özbek, Onur, and Hamit Saruhan. "The effect of vibration and cutting zone temperature on surface roughness and tool wear in eco-friendly MQL turning of AISI D2." *Journal of Materials Research and Technology* 9, no. 3 (2020): 2762-2772.
- [6]. Lopes, José Claudio, Mateus Vinicius Garcia, Roberta Silveira Volpato, Hamilton José de Mello, Fernando Sabino Fonteqe Ribeiro, Luiz Eduardo de Angelo Sanchez, Kleper de Oliveira Rocha, Luiz Daré Neto, Paulo Roberto Aguiar, and Eduardo Carlos Bianchi. "Application of MQL technique using TiO<sub>2</sub> nanoparticles compared to MQL simultaneous to the grinding wheel cleaning jet." *The International Journal of Advanced Manufacturing Technology* 106 (2020): 2205-2218.
- [7]. Gupta, Munish Kumar, Mozammel Mia, GurRaj Singh, Danil Yu Pimenov, Murat Sarıkaya, and Vishal S. Sharma. "Hybrid cooling-lubrication strategies to improve surface topography and tool wear in sustainable turning of Al 7075-T6 alloy." *The International Journal of Advanced Manufacturing Technology* 101 (2019): 55-69.
- [8]. Feng, Xinmin, Cong Meng, Wei Lian, Xiwen Fan, and Jiaxuan Wei. "Optimization analysis of microtexture size parameters of tool surface for turning GH4169." *Ferroelectrics* 607, no. 1 (2023): 186-207.
- [9]. Bargaonkar, Avinash, and Ismail Syed. "Tool wear analysis in AISI 52100 steel machining with sustainable approach." *Materials and Manufacturing Processes* (2024): 1-11.
- [10]. Zou, Yunhe, Shufeng Tang, Shijie Guo, and Xiaojuan Song. "Tool wear analysis in turning inconel-657 using various tool materials." *Materials and Manufacturing Processes* (2024): 1-6.
- [11]. Rosas, José, Hernani Lopes, Bruno Guimarães, Paulo AG Piloto, Georgina Miranda, Filipe S. Silva, and Olga C. Paiva. "Influence of micro-textures on cutting insert heat dissipation." *Applied Sciences* 12, no. 13 (2022): 6583.
- [12]. Mallikarjuna, P., and P. Prasanna. "Comparison of turning process performance using modified cutting inserts under minimum quantity lubrication." *Materials and Manufacturing Processes* 39, no. 5 (2024): 700-710.
- [13]. Bargaonkar, A.; Syed, I. Effect of Coating Material Properties on the Lubrication Performance of Rolling Contacts Under TEHL Regime. *Aust. J. Mech. Eng.* 2022, 2020(2), 352–359. DOI: 10.1080/14484846.2019.1710018 .
- [14]. Karthick, M.; Anand, P.; Meikandan, M.; Siva Kumar, M. Machining Performance of Inconel 718 Using WOA in PAC. *Mater. Manuf. Process.* 2021, 36(11), 1274–1284. DOI: 10.1080/10426914.2021.1905840 .

- [15]. Mahesh, K.; Philip, J. T.; Joshi, S. N.; Kuriachen, B. Machinability of Inconel 718: A Critical Review on the Impact of Cutting Temperatures. *Mater. Manuf. Process.* 2021, 36(7), 753–791. DOI: 10.1080/10426914.2020.1843671 .
- [16]. Ishfaq, K.; Waseem, M. U.; Sana, M. Investigating Cryogenically Treated Electrodes' Performance Under Modified Dielectric(s) for EDM of Inconel (617). *Mater. Manuf. Process.* 2022, 37(16), 1902–1911. DOI: 10.1080/10426914.2022.2065016 .
- [17]. A. Khan and K. Gupta, A Study on Machinability of Nickel-Based Superalloy Using Microtextured Tungsten Carbide Cutting Tools, *Mater. Res. Express*, 2020 <https://doi.org/10.1088/2053-1591/ab61bf>.
- [18]. Gerami, M.; Farahnakian, M.; Elhami Joosheghan, S. Effect of Grooving Textured Tool on the Titanium Chip Morphology. *Mater. Manuf. Process.* 2022, 37(9), 1013–1021. DOI: 10.1080/10426914.2021.2001515.
- [19]. Feng, X.; Meng, C.; Lian, W.; Fan, X.; Wei, J. Optimization Analysis of Micro texture Size Parameters of Tool Surface for Turning GH4169. *Ferroelectrics.* 2023, 607(1), 186–207. DOI: 10.1080/00150193.2023.2198385.
- [20]. Sivaiah, P.; Singh, M.; Chengal Reddy, V.; Meghashyam, P. Processing of 17-4 PH Steel in Turning Operation with Hybrid Textured Tools. *Mater. Manuf. Process.* 2022, 37(3), 241–250. DOI: 10.1080/10426914.2021.2001503.
- [21]. Kumar, V. U.; Raj, D. S. Performance Analysis of Tools with Rake Face Textures Produced Using Wire-EDM in Turning AISI4340. *Mater. Manuf. Process.* 2021, 36(10), 1146–1160. DOI: 10.1080/10426914.2021.1905826.
- [22]. B.V. Chowdary, R. Jahoor, F. Ali Gokool, TJJOME, Optimisation of Surface Roughness when CNC Turning of Al-6061 Application of Taguchi Design of Experiments and Genetic Algorithm. 16 (2):77–91 2019.
- [23]. L. Abhang, Hameedullah MJTJoER (2012) Optimal machining parameters for achieving the desired surface roughness in turning of steel. 9 (1):37-45.
- [24]. Boyer RR (1995) Titanium for aerospace: rationale and applications. *Adv Perform Mater* 2:349–368. doi:10.1007/BF00705316
- [25]. Peters M, Kumpfert J, Ward CH, Leyens C (2003) Titanium alloys for aerospace applications. *Adv Eng Mater* 5:419–427. doi:10.1002/adem.200310095.